Original Paper

Cellular Physiology and Biochemistry

Cell Physiol Biochem 2009;24:585-594

Accepted: August 25, 2009

Bone Marrow Mononuclear Cells Attenuate Interstitial Fibrosis and Stimulate the Repair of Tubular Epithelial Cells after Unilateral Ureteral Obstruction

André L. Barreira[1,*], Christina M. Takiya[2,*], Raquel C. Castiglione[3], Tatiana Maron-Gutierrez[3], Carolina M.L. Barbosa[3] , Débora S. Ornellas[3], Karine S. Verdoorn[3,4], Bernardo M. Pascarelli[5], Radovan Borojevic[2], Marcelo Einicker-Lamas[3,4], Maurilo Leite Jr[1], Marcelo M. Morales[3] and Adalberto Vieyra[3,4]

[1]Faculdade de Medicina and Hospital Universitário "Clementino Fraga Filho", Universidade Federal do Rio de Janeiro, Rio de Janeiro, [2]Instituto de Ciências Biomédicas, Universidade Federal do Rio de Janeiro, Rio de Janeiro, [3]Instituto de Biofísica "Carlos Chagas Filho", Universidade Federal do Rio de Janeiro, Rio de Janeiro, [4]Instituto Nacional de Ciência e Tecnologia em Biologia Estrutural e Bioimagem, Rio de Janeiro, [5]Fundação Oswaldo Cruz, Rio de Janeiro, *These authors contributed equally to this work

Key Words

Bone marrow mononuclear cells • Unilateral ureteral obstruction • Tissue repair • Nephropathies • Adult stem cells

Abstract

The growing number of patients suffering from chronic renal disease is a challenge for the development of innovative therapies. Benefits of cell therapy in acute renal diseases in animal models have been reported but seldom for chronic lesions. We present evidence for the improvement of renal morphology in a model of tubulointerstitial fibrosis. Wistar rats were submitted to unilateral ureteral obstruction (UUO), treated with bone-marrow mononuclear cells (UUO+BMMC) infused via the cava vein, and killed on day 14. Labeled BMMC were seen in renal tissue after 7 days in the group UUO+BMMC. UUO+BMMC also showed a reduction in ED1$^+$ cells and tubular apoptotic cells together with enhanced tubular proliferation. Myofibroblasts were also reduced after BMMC which is consistent with a decrease in collagen deposition (picro Sirius staining) and RT-PCR data showing lower levels of procollagen-I mRNA. Simultaneously, nestin$^+$ cells increased in the interstitium and decreased in the tubules. Double stained nestin$^+$/α-SMA$^+$ cells were present only in the interstitium, and their levels did not change after BMMC infusion. These data indicate a renoprotective effect of BMMC through increased tubular cell regeneration, inhibition of tubular cell apoptosis and partially blocking of the inflammatory and fibrotic events that occur after unilateral ureteral obstruction.

Introduction

The number of patients with chronic kidney disease (CKD) is steadily increasing throughout the world, with a prevalence of 15.2% of the adult US population (NHANES study) [1]. Presently, treatments primarily concentrate on dialysis and transplantation. The former

KARGER

Fax +41 61 306 12 34
E-Mail karger@karger.ch
www.karger.com

1015-8987/09/0246-0585$26.00/0

Accessible online at:
www.karger.com/cpb

Adalberto Vieyra and Marcelo M. Morales
Instituto de Biofísica Carlos Chagas Filho
Universidade Federal do Rio de Janeiro, 21941-902 Rio de Janeiro (Brazil)
Tel. +55 21 2562-6520, Fax +55 21 2280-8193
E-Mails avieyra@biof.ufrj.br, mmorales@biof.ufrj.br

is facing increasingly financial constraints, whereas transplantation is not being universally applied. Hence, alternative strategies have been pursued to develop new therapies for chronic renal failure.

In the last decade, the use of bone marrow cells has emerged as a new approach to treatment. Chimeric animals obtained by infusing genetically marked bone marrow mononuclear cells (BMMC) in diverse models of kidney injury have provided new and controversial insights into kidney remodeling. Less than a decade ago, Ito and coworkers [2] and Imasawa and coworkers [3] were the first to show that BMMC differentiate into mesangial cells in a glomerulonephritis model. Rookmaaker and coworkers [4], using the same model of glomerular injury, demonstrated the transdifferentiation of BMMC into mesangial and glomerular endothelial cells. However, the contribution of bone marrow cells to the recovery of tubular injury remains controversial. Transdifferentiation of BMMC into renal proximal tubular cells has been demonstrated in sex-mismatched clinical kidney transplants. Using fluorescent *in situ* hybridization and immunohistochemistry, Y-chromosome-positive cells expressing tubular cell markers were detected in female kidney allografts at frequencies from 1 to 20% [5]. Three-dimensional confocal microscopic analysis of ischemia/reperfusion injured kidneys treated with enhanced green fluorescent protein (EGFP) unfractionated BMMC had far fewer tubular cells containing EGFP than had previously been reported [6]. Also BMMC did seem not to transdifferentiate into tubular cells in these injured kidneys, as shown using either total bone marrow cells or mesenchymal stem cells [7, 8]. When it did occur, it seemed to be at an extremely low frequency [9-11], as has been reported in other animal models of tubular necrosis, e.g. toxic injuries [12-15].

Notwithstanding the mechanism underlying the benefit caused by BMMC infusion, a clear relationship exists between the severity of renal damage and the extent of tubular BMMC engraftment [11]. This applies to clinical situations where higher frequencies of host-derived cells inside kidney tubules have been correlated with episodes of acute tubular necrosis or rejection [5]. However, these observations refer to situations in which renal repair occurs after an acute insult; to date few studies have addressed the role of BMMC in steadily progressive disease.

Our investigation addresses the role of heterologous BMMC in the histological pattern of inflammation, fibrosis, epithelial cell proliferation and apoptosis in unilateral ureteral obstruction (UUO) using a rat model. Particular attention has been paid to key cellular and molecular markers of inflammation and fibrosis, as well as tubular regeneration in this model of chronic tubulointerstitial damage and progressive loss of renal tissue.

Materials and Methods

Animals and experimental protocol

Sixteen adult male Wistar rats, aged 3 months and weighing ~250 g, underwent left ureteral obstruction or served as sham-operated controls. The rats were anesthetized by intraperitoneal injection of ketamine (50 mg/kg) and xylazine (5 mg/kg). The left ureter was ligated using 4-0 silk at 2 points and sectioned between the ligatures and the rats were kept in standard cages. They were divided into 4 groups of 4 animals: (i) sham-operated infused with buffered saline solution (BSS) (SHAM), (ii) sham infused with BMMC (SHAM+BMMC), (iii) unilateral ureteral obstruction injected with BSS (UUO), and (iv) unilateral ureteral obstruction infused with BMMC (UUO+BMMC). The sham-operated animals underwent identical surgical procedures, except that the left ureter was manipulated without ligation and sectioning. The groups SHAM+BMMC and UUO+BMMC received the cells through the inferior cava vein immediately after the surgery. All groups received antibiotics in their drinking water (0.1% amoxicillin [Medley, Sumaré, Brazil] and 0.015% enrofloxacine [Schering-Plough, Cotia, Brazil]) for 14 days. The rats were kept in a 12-h light/dark cycle at 25°C and fed standard rat chow and water *ad libitum*. After 14 days, the animals were killed under anesthesia and the kidneys removed.

Two extra groups (SHAM and UUO+BMMC) were used for experiments in which BMMC were labeled to trace the localization of these cells in kidney after UUO. These animals were killed on day 7 of UUO because remodeling of tubular cells (dedifferentiation, apoptosis and proliferation) is already high at this point [16]. Control groups, i.e. rats not submitted to any surgical procedure were not included in this study, since previously we had found no histological difference between control and sham groups [17]. All experimental procedures were conducted in accordance with "The Guide for Care and Use of Laboratory Animals" [DHHS Publication Nº (NIH) 85-23, Office of Science and Health Reports, Bethesda, MD 20892] and followed the recommendations of the American Veterinary Medical Association Guidelines on Euthanasia, 2007 (both available online at http:\\www.nih.gov). All procedures were approved by the Committee for Experimental and Animal Ethics at the Federal University of Rio de Janeiro.

Preparation of BMMC

Eight-week male Wistar rats were killed and both femurs and tibias were excised and BMMC were collected by flushing marrow cavities with Dulbecco's modified Eagle's medium (DMEM, Gibco, Grand Island, NY). Mononuclear cells were isolated using a density gradient (Ficoll/Paque, GE Healthcare, Uppsala, Sweden) and resuspended in DMEM. After

centrifugation, cells were washed with BSS and the number of cells in each sample was determined with a Neubauer chamber.

Infusion of BMMC

BMMC were injected into the inferior cava vein after suspension in 1 mL BSS. Approximately 2×10^7 cells were given per rat. The same volume of BSS was infused into the control animals.

Tracing the BMMC

BMMC were incubated with CellTrace™ Far Red DDAO-SE (Invitrogen, cat. C-34553, Eugene, OR), according to the manufacturer's instructions and infused into SHAM and UUO+BMMC rats (2 rats per group). The animals were sacrificed 7 days after BMMC infusion and perfused with sterile saline containing heparin (10 U/mL) via the left cardiac ventricle followed by 4% (w/v) buffered paraformaldehyde (PF) solution and then with a 1:1 mixture of PF and 10% (w/v) sucrose. The kidneys were removed, cryopreserved in 30% (w/v) sucrose in PBS (phosphate buffered saline), embedded in Tissue-Tek OCT compound (Tissue Tek®, Sakura Finitek USA, Torrance, CA) and frozen at -80°C. Frozen sections (10 µm thick) were obtained, collected onto poly-L-lysine coated slides and fixed with cold acetone. The sections were washed with PBS and incubated with 5% (w/v) bovine serum albumin (BSA) in PBS before being stained with 10 µg/mL 4'-6-diamidino-2-phenylindole (DAPI, 10 µg/mL, Santa Cruz Biotechnology, Santa Cruz, CA). The sections were washed in PBS and coverslipped with Vectashield mounting medium (Vector Laboratories, Burlingame, CA). A Zeiss confocal microscope LSM 510 META NLO was used to visualize Far Red DDAO, with excitation at 646 nm and emission at 659 nm.

Tissue preparation

Animals were perfused with sterile saline containing heparin (10 U/mL) via the left cardiac ventricle, followed by infusion with PF. The kidneys were removed and sectioned midfrontally into 2 pieces, immersed in Bouin's fixative and embedded in paraffin. Sections 4 µm thick were cut and stained with hematoxylin-eosin (HE) and periodic acid-Schiff reagent (PAS) to visualize basement membrane, plus a modified picro-Sirius red technique for collagen [18]. Immunohistochemical procedures on the paraffin-embedded sections involved: (i) a mouse monoclonal antibody against α-smooth muscle actin (α-SMA) (Dako, Carpinteria, CA) to detect myofibroblasts, (ii) a mouse monoclonal antibody against rat ED-1 to detect macrophages (AbD Serotec, Raleigh, NC), (iii) a mouse monoclonal antibody against proliferating cell nuclear antigen (PCNA, Dako), and (iv) a mouse monoclonal antibody against rat nestin (AbD Serotec). Antibodies were visualized with the Dako LSAB® 2 system HRP kit (Dako) using diaminobenzidine as the chromogenic substrate (Liquid DAB, Dako).

For co-localization of α-SMA and nestin, paraffin sections were dewaxed, immersed in 5% (w/v) borohydroxide and incubated in PBS containing 5% (w/v) BSA, 0.01% (w/v) gelatin, 0.01% (w/v) Tween-20 (w/v) and 0.05% (w/v) Triton X-100. They were incubated overnight in a humid chamber (4°C) with a mouse monoclonal α-SMA antibody which had previously been biotinylated using the ARK kit from Dako following the manufacturer's instructions. In a subsequent step, they were washed with PBS containing 0.25% (w/v) Tween-20 and incubated with streptavidin-Cy3 (Sigma). Endogenous biotin was inhibited with a blocking kit from Vector according to the manufacturer's instructions. Finally, the sections were incubated with a monoclonal antibody against nestin (AbD Serotec), which was visualized with a goat anti-mouse IgG conjugated with Alexa 488 (Invitrogen Co, Carlsbad, CA), washed and incubated with TOPRO3 iodide (Invitrogen Co) to stain the nuclei.

Apoptosis assay

Apoptotic tubular cells in kidney tissue were measured by the terminal deoxytransferase uridine triphosphate nick end-labeling technique (TUNEL), using the ApopTag® Peroxidase in situ apoptosis detection kit (Chemicon International, Temecula, CA). The reaction was performed according to the manufacturer's instructions.

Histomorphometry

For histomorphometry, an image analysis system composed of a digital camera (Evolution, Media Cybernetics Inc., Bethesda, MD) coupled to a light microscope (Eclipse 400, Nikon) was used. High quality images (2048×1536 pixels buffer) were captured with Pro Plus 4.5.1 software (Media Cybernetics). All the quantifications were done by a single observer.

Collagen, myofibroblast (α-SMA) and ED1$^+$ density surfaces

Picro Sirius red, α-SMA and ED1 stained sections were used to obtain 15 (Picro Sirius) or 10 (other markers) photomicrographs from renal tissue with a 40× objective lens. The areas were randomly chosen, although fields containing medium-sized blood vessels, glomeruli or renal capsule were carefully avoided. The results represent the percentages of collagen, α-SMA and ED1 immunodetected in the total cortical or medullar surface and are expressed as mean±SEM.

Quantification of nestin$^+$ cells in kidney interstitium and tubules

Histological sections stained for nestin were used to capture 10 microscopic fields from the renal tissue as above. The results represented the percentage of nestin reactive cells present either in the interstitium or inside tubules per the total number of tubular or interstitial cells. Results are expressed as mean±SEM.

Quantification of double-stained (nestin$^+$/α-SMA$^+$) cell populations in kidney interstitium

Histological sections double-stained for nestin (using fluorochrome Alexa 488) and α-SMA, (using fluorochrome Alexa 586) were examined to quantify the number of nestin$^+$ and double-stained (nestin$^+$/α-SMA$^+$) cell populations. Ten randomly captured microscopic fields (objective 63×) were obtained from each kidney sections. Results are expressed as mean±SEM.

Proliferation (% PCNA⁺ cells) and apoptotic (% apoptotic cells) indices

The number of cells positive for PCNA, or the apoptag assay divided by the total number of tubular cells gave respectively the proliferation or apoptotic index. Results are expressed as mean±SEM.

Extraction of total RNA

Total RNA was extracted from rat kidneys using Trizol® reagent (Gibco BRL, Gaithersburg, MD), following the protocol recommended by the manufacturer. The isolated RNAs were treated with 1 U/µL RNase-free DNase I (Gibco BRL) for 30 min to eliminate contaminating genomic DNA. Autoclaved diethylpyrocarbonate-treated water was used to dissolve the RNA, which was quantified by spectrophotometric absorbance at 260 nm.

Semi-quantitative reverse transcription and polymerase chain reaction (RT-PCR)

The technique was chosen for comparison of renal mRNA expression for each studied gene in experimental animals compared to control group (SHAM, taken as 100% [19]). First-strand complementary deoxyribonucleic acid (cDNA) was prepared using 1 µg of total RNA. The total RNAs were primed with oligo(dT) primer and reverse-transcribed using SuperScript™ (Gibco BRL) at 37°C for 60 min. The negative control corresponded to a 1 µg aliquot of total RNA used for cDNA synthesis in the absence of the RT enzyme, and was called RT(-). The cDNA synthesis reaction was interrupted by DNA extraction using a mixture of phenol, chloroform and isoamyl alcohol (25:24:1), followed by precipitation with 7.5 M ammonium acetate in ethanol for 24 h at -20°C. Finally, the cDNA was resuspended in 5 µL deionized water.

In the PCR reaction, cDNAs were used in the presence of 2.5 U Taq polymerase (Gibco BRL), 0.12 µM of the primers for pro-collagen I (PC-I), pro-collagen III (PC-III) and glycerol 3-phosphate dehydrogenase (GAPDH), 0.2 µM of each nucleotide, and 2.5 µL of a commercial buffer 10× (Gibco BRL) containing 1.5 mM $MgCl_2$. PCR was as follows: initial denaturation at 94°C for 4 min, and 36 cycles of denaturation (94°C, 1 min), annealing (58°C, 1 min) and extension (72°C, 1 min). The reaction ended with extension for 10 min at 72°C. All pairs of primers used were designed in different exons for each studied gene. The primers used in the PC-I PCR reactions were 5'-GGC TTC AAA GGC ATT CGA G-3' and 5'-GCG GTG AAG AAG GAA AGA G-3', which produced a DNA segment of 620 bp. The primers used for the PC-III PCR reactions were 5'-CTG CCA TTG CTG GAG TTG-3' and 5'-GCA GCC ATC CTC TAG AAC-3', which produced a DNA segment of 615 bp. As an internal control for both reactions, rat GAPDH primers 5'-GTC TTC ACC ACC ATG GAG-3' and 5'-CAT GAC AAC TTT GGC ATC-3' were used, which produced a segment of 211 bp. The identities of the amplified products were confirmed by molecular size determination on agarose gel electrophoresis (1.5% agarose in buffer containing 40 mM Tris/acetate and 1 mM EDTA) and visualized with ethidium bromide (0.5 µg/L) under ultraviolet irradiation. The PC-I, PC-III and GAPDH bands were analyzed by densitometry (Scion Image Alpha 4.0.3.2). Expression was normalized by dividing the PC-I or PC-III values by the corresponding internal control values (GAPDH) amplified in the same reaction tube [20].

The optimal PCR conditions that yielded a single band on agarose gel electrophoresis were determined for each gene (PC-I, PC-III). Total rat kidney RNAs were used for RT-PCR amplification of the collagen primer pair together with GAPDH primers in the same reaction tube to determine whether the method was semi-quantitative. All reactions included a negative control (cDNA replaced with double-distilled water).

Statistical analysis

When appropriate, results are expressed as mean±SEM. Statistical analysis was performed using ANOVA followed by the Student Neuman Keuls test. $P<0.05$ was considered statistically significant.

Results

BMMC become recruited to the renal interstitium after UUO

Migration of CellTrace-stained BMMCs to the obstructed kidney was investigated 7 days after transplantation (Fig. 1). They accumulated in the interstitium of both the cortico-medullary transition area and the medulla (Fig. 1A), but were sparsely populated inside the tubular epithelial lining (Fig. 1B). Cells were also seen inside the glomeruli (Fig. 1C). Very few BMMC were found in the interstitium of contralateral kidneys, whereas no labeling occurred inside the tubular epithelium and in the glomeruli from UUO (Fig. 1D-F) or in the non-operated controls (not shown).

Histopathological analysis

The kidneys exhibited some parenchymal atrophy 14 days after obstruction. This was partially prevented in BMMC-treated animals, where tubular dilatation (arrow heads) as well as papillary distortion (asterisk) was less prominent than in the UUO rats (Fig. 2), indicating that BMMC reduced the morphological signs of tissue damage. This was also true for tubular cell proliferation as judged by the PCNA index, which was significantly higher in the BMMC-treated rats than in the UUO group (44.9±2.9% and 19.5±2.9%, respectively; Fig. 3). In addition, the number of apoptotic tubular cells was significantly lower in the BMMC-treated group than in the UUO group (5.6±1.9% and 23.2±3.1%, respectively; Fig. 4). The combined results from Fig. 3 and 4 reflect clear renoprotection elicited by BMMC infusion.

We went on to evaluate the influence of BMMC infusion on the progression of inflammatory and fibrotic

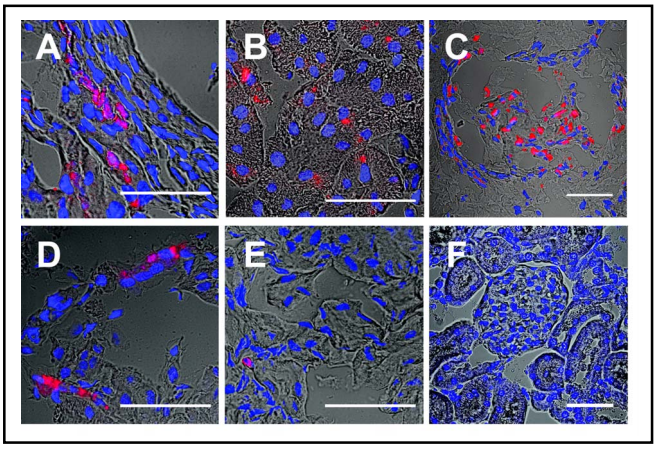

Fig. 1. Tracing BMMC in kidney sections 7 days after infusion. The BMMC cytosol (red) was stained with Cell Trace™ Far Red DDAO-SE and the nuclei with DAPI (blue). Upper panels: representative images from obstructed kidneys; lower panels: contralateral kidneys. (A,D) Interstitial localization. (B,E) Tubular localization. (C,F) Glomerular localization. Bars = 50 µm.

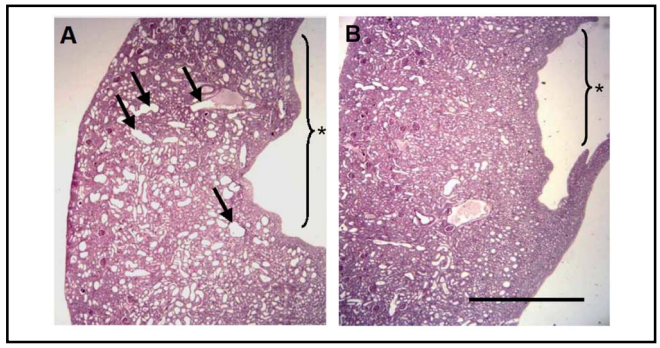

Fig. 2. Photomicrography of HE-stained kidney sections from UUO and UUO+BMMC rats. (A) Kidney section from UUO showing dilated renal tubules (arrows) and deformations in the renal calicial zone (asterisk region). (B) Kidney section from UUO+BMMC showing attenuation of tubular dilatation and less deformation in the calicial region. Bar = 10 µm.

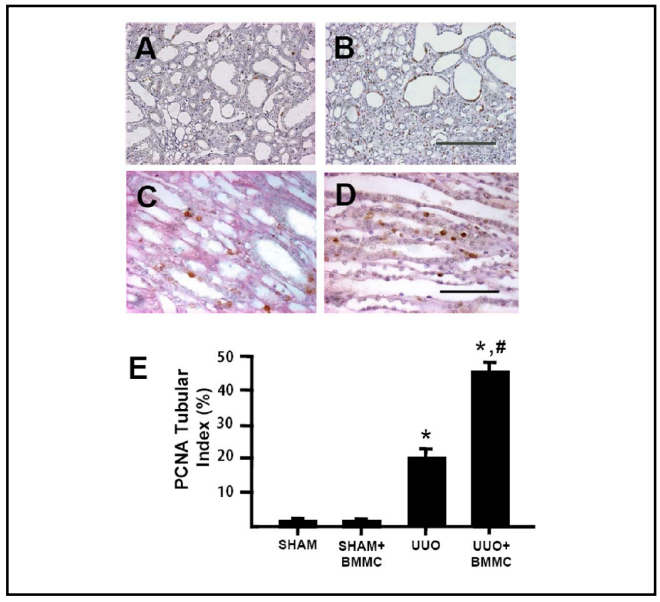

Fig. 3. BMMC administration induces tubular cell proliferation in UUO. The percentage of nuclei reactive to PCNA was calculated in cortical and medullary tubular cells. Representative immunostaining of corticomedullary transition from UUO (A) and UUO+BMMC (B) (Bar = 400 µm). Representative medullary immunostaining from UUO (C) and UUO+BMMC (D) (Bar = 100 µm). (E) Quantification of $PCNA^+$ cells in the experimental conditions indicated on the abscissa. Columns indicate means ± SEM of 40 captured images (20 from cortex and 20 from medulla) from each kidney in the different experimental groups ($n = 4$). * $P < 0.001$ *vs* SHAM and SHAM+BMMC. # $P < 0.001$ *vs* UUO.

processes, which are closely related to the pathophysiology of UUO. The surface density of the inflammatory macrophage marker (ED1 antigen) was significantly lower after BMMC infusion than in the UUO group (0.71±0.08% and 1.11±0.20%, respectively; Fig. 5). The myofibroblast surface density (α-SMA) was also significantly lower in the UUO+BMMC group (3.20±0.31%) than the UUO group (6.54±0.87%; Fig. 6), although fibrosis was still evident compared to the normal and very low values in the SHAM group. Collagen deposition was also significantly lower in the UUO+BMMC group, as shown by picro Sirius-staining (Fig. 7). The intense collagen deposition in the tubular basement membranes and the interstitial space in the UUO group (13.23±0.67%; Fig. 7A) was clearly attenuated by BMMC treatment (8.11±0.27%), mainly in the deformed papillary region (Fig. 7B,C). This BMMC-induced anti-fibrotic and anti-inflammatory pattern was consistent with the collagen mRNA data (see below).

Nestin is considered a marker for neuroepithelial stem cells but can occur in non-neural and progenitor cells, suggesting that it may indicate multi-potentiality and regenerative potential [21]. Nestin is expressed during kidney development [22, 23]. During differentiation, its expression is downregulated, persisting only in the glomeruli in adult life [22-24]. The reappearance of nestin in tubules suggests either its role in migration of stem/progenitor cells during tubular regeneration after injury [25, 26], or in epithelial mesenchymal transition [27]. Therefore nestin was followed by immunostaining to evaluate the participation of adult renal stem/progenitor cells in UUO, phenotypic modification of renal tubules (dedifferentiation), or transdifferentiation of interstitial fibroblast after BMMC infusion. In the controls, nestin

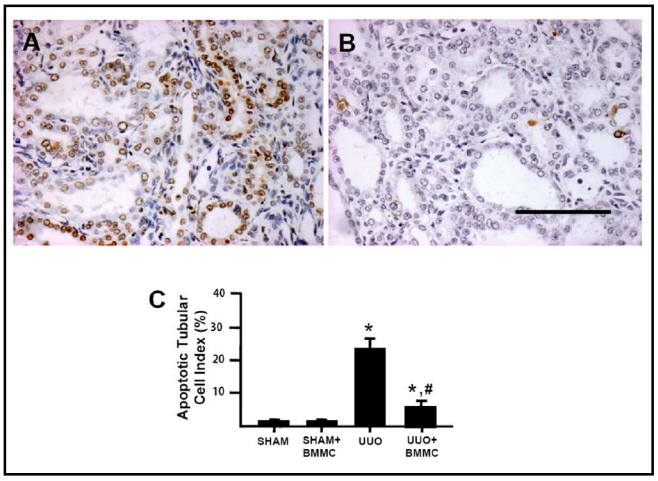

Fig. 4. BMMC administration decreases apoptosis in tubular cells. Apoptotic cells were counted by the TUNEL technique. (A) Representative UUO cortical image. (B) Representative UUO+BMMC cortical image. (C) Apoptotic tubular cells in the experimental conditions shown on the abscissa were quantified as described in the legend to Fig. 3. * P <0.001 *vs* SHAM and SHAM+BMMC. # P <0.001 *vs* UUO. Bar = 100 µm.

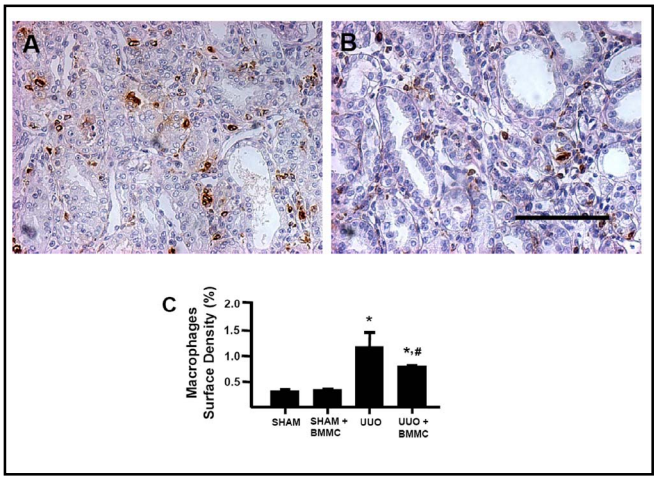

Fig. 5. BMMC decrease macrophage infiltration in UUO. Surface density of ED1^{+} macrophages was evaluated as described in Materials and Methods. (A) Representative image of UUO kidney cortex. (B) Representative image of UUO+BMMC kidney cortex. (C) Macrophage surface density in the experimental conditions indicated on the abscissa was quantified (means ± SEM) from the acquired images as described in the legend to Fig. 3. * P <0.001 *vs* SHAM and SHAM+BMMC. # P < 0.05 *vs* UUO. Bar = 100 µm.

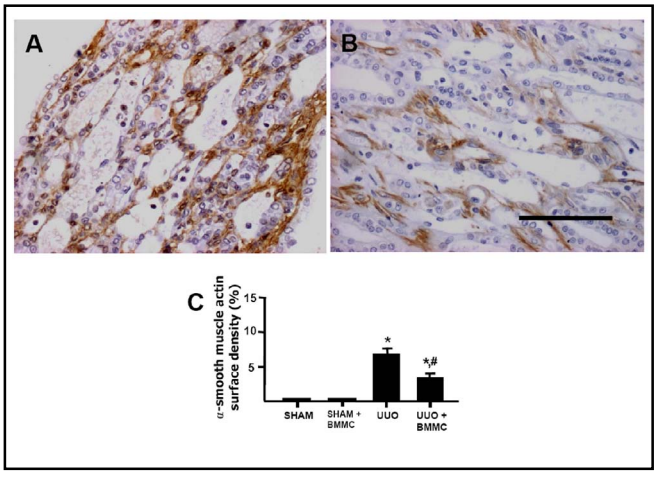

Fig. 6. α-SMA immunoexpression is partially blocked by BMMC in UUO. Myofibroblast immunolocalization and surface density of α-SMA in kidney medulla were evaluated (see Materials and Methods). (A) Representative UUO image. (B) Representative image of UUO+BMMC image. (C) Graphic representation (means ± SEM) of α-SMA surface density in the experimental conditions indicated on the abscissa. Numbers of acquired images and animals per group were as same as in the legend to Fig. 3. *P <0.001 *vs* SHAM and SHAM+BMMC. # P <0.05 *vs* UUO. Bar = 100 µm.

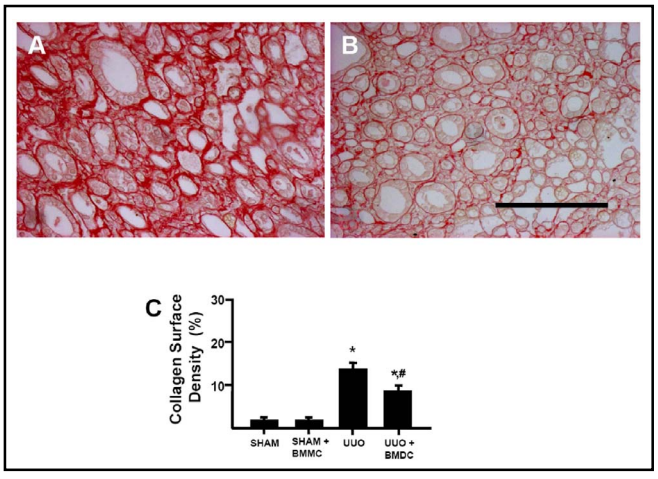

Fig. 7. BMMC reduce collagen deposition in UUO. Picro-Sirius staining of kidney sections and evaluation of collagen surface density were carried out. (A) Representative image of UUO medulla. (B) Representative image of UUO+BMMC medulla. (C) Graphic representation (means ± SEM) of collagen surface density in the experimental conditions indicated on the abscissa was as described in the legend to Fig. 3. * P <0.001 *vs* SHAM and SHAM+BMMC. # P <0.001 *vs* UUO. Bar = 100 µm.

was only seen in glomerular podocytes, as in [28]. We found that nestin-positive cells were present in the interstitial compartment after UUO, with either an elongate or stellate shape located at a submembranar position below the tubular basement membrane, or they were immersed in the interstitial matrix (Fig. 8A). In the

Fig. 8. BMMC influence the distribution of adult progenitor cells in the interstitium and tubule in opposite ways. (A) Interstitial nestin$^+$ cortical cells in UUO. (B) Increased interstitial nestin$^+$ cells in UUO+BMMC. (C) Percentage of interstitial nestin$^+$ cells with respect to the total number of nestin$^+$ cells. (D) Tubular nestin$^+$ cortical cells in UUO. (E) Decreased tubular nestin$^+$ cortical cells in UUO+BMMC. (F) Percentage of tubular nestin$^+$ cells with respect to the total number of nestin$^+$ cells. In C and F, the findings were quantified as in Fig. 3. * P <0.001 *vs* UUO (C), (F). (A) and (B) Bar = 50 µm. (D) and (E) Bar = 100 µm.

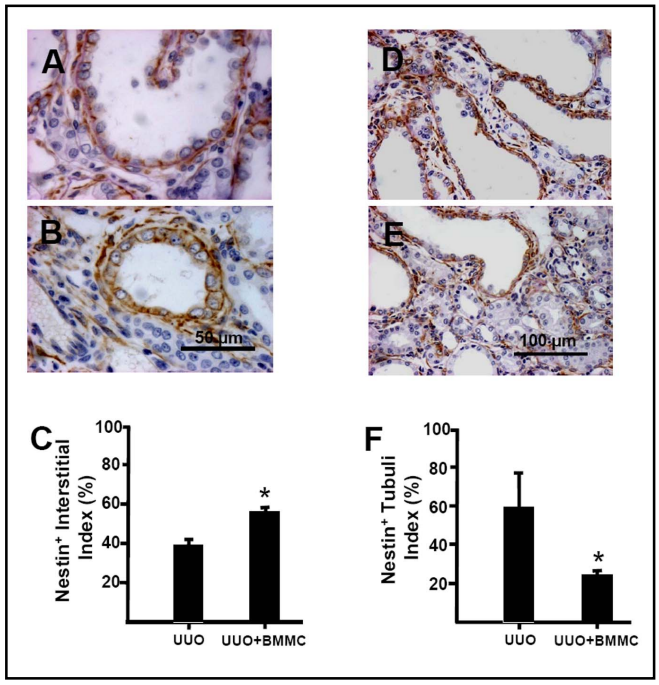

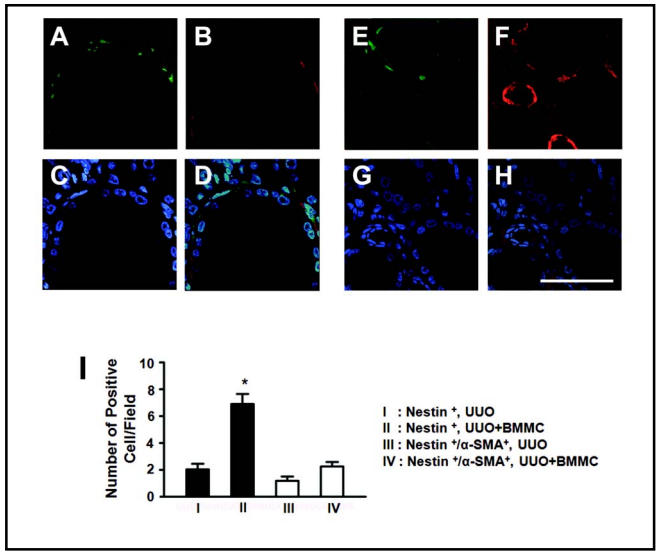

Fig. 9. Minor contribution of adult renal progenitor cells to myofibroblast appearance after BMMC infusion. Co-localization of nestin$^+$ and α-SMA$^+$ were measured in interstitial cells. Kidney sections from UUO+BMMC group showing: (A) Nestin$^+$ cells (green), (B) α-SMA$^+$ cells (red), (C) Nuclei of cells (blue) and (D) Merge. Kidney sections from UUO group showing: (E) Nestin$^+$ cells (green), (F) α-SMA$^+$ cells (red), (G) Nuclei of cells (blue) and (H) Merge. (I) Graphic representation of nestin$^+$ and double-stained (nestin$^+$/α-SMA$^+$) cells in UUO (I and III, respectively) and UUO+BMMC groups (II and IV, respectively), as indicated on the abscissa (n = 5 rats per group; 50 fields). There was a significant increase in nestin$^+$ cells in UUO+BMMC group (* P <0.001) with respect to the other 3 populations of cells. However, there was no statistical difference in the number of nestin$^+$/α-SMA$^+$ cell population between the UUO+BMMC and UUO groups. Bar = 50 µm.

UUO+BMMC group, the amount of interstitial nestin$^+$ cells was significantly increased relative to the UUO group (56.4±1.8% *vs* 39.3± 2.9%, respectively; Fig. 8B,C). After UUO, nestin was predominantly expressed in dilated tubules at the corticomedullary region where membrane reactivity in the basolateral domains was depicted (Fig. 8D). With BMMC infusion, the number of tubule nestin reactive cells significantly diminished in comparison with UUO animals (40.0±5.2% *vs* 24.1±2.0%; Fig. 8E,F).

The amount of nestin$^+$ cells that were also able to express the marker of myofibroblasts was determined. Despite a huge increase in nestin$^+$ cells after BMMC infusion (Fig. 9A-D, I), the amount of double-stained nestin$^+$/α-SMA$^+$ cells was unaltered after BMMC infusion (1.18±0.32 *vs* 2.25±0.33, respectively; Fig. 9E-I). Together the present results demonstrate that BMMC infusion favored the accumulation of a nestin$^+$ cell population in the peritubular compartment, which could represent the migration of stem/progenitor cells. Interestingly, BMMC infusion did not contributed to the increase in the number of tubular dedifferentiated cells and did not give raise to the myofibroblast population.

Expression of pro-collagen I and III mRNA

The development of fibrotic injury is associated with variations in the expression of at least collagen I and III, and the increased ratio between newly deposited collagen such as indicated by the levels of PC-I and PC-III. The increased ratio between PC-I and PC-III indicates the evolution towards a fibrotic stage [29, 30] and, therefore, the only aim of the experiments depicted in figure 10 was to investigate the influence of BMMC in this ratio. Semi-quantitative RT-PCR showed that the expression of PC-I mRNA differed between UUO and UUO+BMMC groups. Densitometric analysis of the bands corresponding to PC-I showed that UUO group presented ~150% of the PC-I mRNA in controls, BMMC treatment significantly decreased these levels (Fig. 10A). SHAM rats were not statistically different from sham rats treated

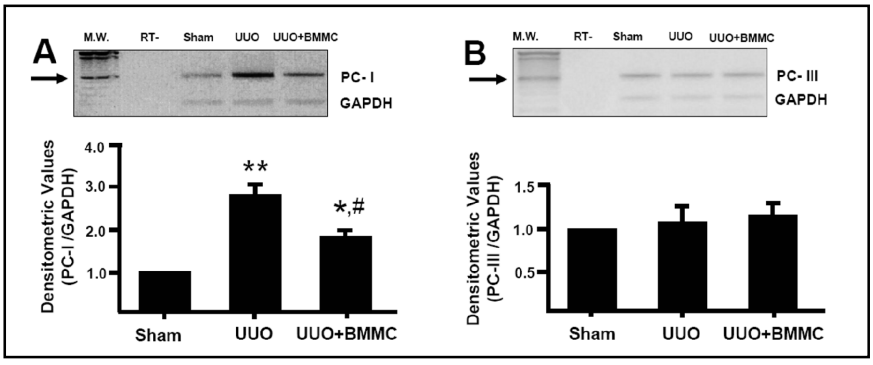

Fig. 10. Differential expression of procollagen I and III mRNAs in UUO, without and with BMMC administration. mRNA expression was evaluated by semi-quantitative RT-PCR. (A) Procollagen-I. Upper panel: Representative agarose gel electrophoresis of the RT-PCR products. Standards of ~620 and ~211 bp are indicated. RT-, synthesis reaction without reverse transcriptase. Lower panel: Quantification of the densitometric values obtained from the ratio PC-I/GAPDH (mean ± SEM, n = 3) in the three experimental conditions indicated on the abscissa. *P <0.05 *vs* SHAM; ** P <0.01 *vs* SHAM; $^{\#}$ P <0.05 *vs* UUO. (B) Procollagen III. Upper panel: Representative agarose gel electrophoresis of the RT-PCR products. Standards of ~615 and ~211 bp are indicated. RT-, the same as in A. Lower panel: Quantification of the densitometric values obtained from the ratio PC-III/GAPDH (means ± SEM, n = 3) under the 3 experimental conditions indicated on the abscissa. No differences were found.

with BMMC (data not shown). No differences in the pattern of PC-III mRNA expression were observed among the groups (Fig. 10B).

Discussion

The increasing number of renal patients worldwide has compelled nephrologists and scientists to search for new therapies that slow down this epidemic disease [31, 32]. Investigations have focused on development of an effective cell therapy, which promised some hope for certain well known nephropathies [33] and other diseases [34]. The UUO model is characterized by a progressive loss of renal tubules and a sustained inflammatory and fibrogenic response [recently reviewed in 30]. We have demonstrated that exogenous BMMC significantly attenuate tubular loss by increasing tubular regeneration and decreasing apoptotic death. Furthermore BMMC infusion improved the inflammatory and fibrogenic processes, despite the persistence of the UUO-induced injury. This study is novel in that it shows the presence of infused BMMC in the tissue of the obstructed kidney after 7 days of UUO (Fig. 1).

Among the proposed mechanisms of action of administered bone marrow-derived cells in kidney repair, the hypothesis of transdifferentiation of these cells into organ-specific phenotypes has been weakened. When repair occurs, it is minimal and not sufficient to explain the regeneration or protection observed [8, 10, 35]. One of the proposed mechanisms for tubular regeneration suggests that new cells appear from the migration and proliferation of stem/progenitor cells of the adult tissue, which apparently exist in the renal papilla [25, 36] or perhaps the individual tubular segments [7, 8]. According to Oliver and coworkers [25] and Patschan and coworkers [36], tubular regeneration in the ischemia/reperfusion model seems to be dependent on the proliferation and migration to the S3 segment of the injured proximal tubules of stem/progenitor cells from the renal papilla [25, 36]. Characterization and migratory behavior of these kidney stem/progenitor cells has already been demonstrated by using nestin as the marker. There is strong evidence that nestin labels undifferentiated progenitor cells since this protein is a multilineage marker [21] which appears during kidney development, although it is downregulated in adult life [22, 23]. More recently repopulating mesangial nestin$^+$ cells were seen in the anti Thy-1 nephritis model [37]. Therefore the re-expression of nestin in tubular cells and in the interstitium in our model (Fig. 8) could represent stem/progenitor cells migration.

The lower detection of ED1$^+$ macrophages (Fig. 5) also supports the view that a decrease in macrophage population probably interferes with a critical event in the progression of kidney lesions toward fibrosis [38], and that it is also an important effect elicited by BMMC. In several models of kidney disease, infusion of bone marrow cells led to attenuation of inflammation, probably due to secretion of different cytokines and growth factors [39-41], and this could have occurred in our experiments, given the diminished macrophage infiltration. In addition, the significant increase in PCNA$^+$ cells within the tubules (Fig. 3) and the decrease in tubular cell apoptosis (Fig. 4) in the UUO+BMMC group strengthen the view that BMMC infusion promotes a renoprotective effect. The effects of BMMC seem to be elicited through some paracrine or endocrine action, a mechanism that has been described for mesenchymal stem cells (MSC) [41], which

represents a minor subpopulation of the BMMC [42]. Among all mediators secreted by MSC, those that seem to be renoprotection are IGF-1, HGF and VEGF [39-41].

Epithelial-mesenchymal transition occurs in UUO [43, 44] and is responsible for the appearance of myofibroblasts [44-46]. However, Iwano and coworkers [44] have demonstrated that myofibroblasts could originate from bone marrow in a mouse model of UUO, raising the risk of enhancing fibrosis, even though these myfibroblasts were non-functional [47, 48]. In a model of chronic ciclosporine nephropathy, Ahn and coworkers [48] showed an increase in nestin expressing cells in renal interstitium which correlates with increased fibrosis. We found, however, that BMMC ameliorated rather than worsened tissue fibrosis. Reduction in the mRNA of PC-I (Fig. 10) is also in line with the weakening of fibrotic deposition. Colocalization of nestin and α-SMA staining did not seem to increase in UUO after BMMC, despite a huge increase in the interstitial nestin$^+$ cell population (Fig. 9), which clearly indicates, at least in our model, that epithelial/ mesenchymal transition is not enhanced by BMMC administration.

In conclusion, we have demonstrated that the infusion of BMMC in a model of chronic tubulointerstitial injury decreased both collagen deposition and the myofibroblast population, associated with a renoprotective role with enhanced proliferation and reduced apoptosis of tubular cells. These synergistic processes ultimately lead to less inflammation and fibrosis in the kidney, tissue regeneration and renoprotection after UUO. Our results also suggest that BMMC helps to recruit progenitor cells through a paracrine mechanism that remains to be elucidated.

Acknowledgements

This work is supported by grants from the Ministério da Ciência e Tecnologia/CNPq/MS/DECIT (552162/2005-1) and FAPERJ (E-26/110.287/2007) to A. Vieyra. The authors acknowledge the required English style corrections by BioMedES (UK).

References

1 U.S. Renal Data System, USRDS 2008 Annual Data Report: Atlas of Chronic Kidney Disease and End-Stage Renal Disease in the United States, National Institutes of Health, National Institute of Diabetes and Digestive and Kidney Diseases, Bethesda, MD, 2008.

2 Ito T, Suzuki A, Imai E, Okabe M, Hori M: Bone marrow is a reservoir of repopulating mesangial cells during glomerular remodeling. J Am Soc Nephrol 2001;12:2625-2635.

3 Imasawa T, Utsunomiya Y, Kawamura T, Zhong Y, Nagasawa R, Okabe M, Maruyama N, Hosoya T, Ohno T: The potential of bone marrow-derived cells to differentiate to glomerular mesangial cells. J Am Soc Nephrol 2001;12:1401-1409.

4 Rookmaaker MB, Smits AM, Tolboom H, Van 't Wout K, Martens AC, Goldschmeding R, Joles JA, Van Zonneveld AJ, Gröne HJ, Rabelink TJ, Verhaar MC: Bone-marrow-derived cells contribute to glomerular endothelial repair in experimental glomerulonephritis. Am J Pathol 2003;163:553-562.

5 Poulsom R, Forbes SJ, Hodivala-Dilke K, Ryan E, Wyles S, Navaratnarasah S, Jeffery R, Hunt T, Alison M, Cook T, Pusey C, Wright NA: Bone marrow contributes to renal parenchymal turnover and regeneration. J Pathol 2001;195:229-235.

6 Toyokawa H, Nakao A, Stolz DB, Romanosky AJ, Nalesnik MA, Neto JS, Kaizu T, Demetris AJ, Murase N: 3D-confocal structural analysis of bone marrow-derived renal tubular cells during renal ischemia/reperfusion injury. Lab Invest 2006;86:72-82.

7 Duffield JS, Park KM, Hsiao LL, Kelley VR, Scadden DT, Ichimura T, Bonventre JV: Restoration of tubular epithelial cells during repair of the post ischemic kidney occurs independently of bone marrow–derived stem cells. J Clin Invest 2005;115:1743-1755.

8 Lin F, Moran A, Igarashi P: Intrarenal cells, not bone marrow-derived cells, are the major source for regeneration in post ischemic kidney. J Clin Invest 2005;115:1756-1764.

9 Lange C, Togel F, Ittrich H, Clayton F, Nolte-Ernsting C, Zander AR, Westenfelder C: Administered mesenchymal stem cells enhance recovery from ischemia/reperfusion-induced acute renal failure in rats. Kidney Int 2005;68:1613-1617.

10 Tögel F, Hu Z, Weiss K, Isaac J, Lange C, Westenfelder C: Administered mesenchymal stem cells protect against ischemic acute renal failure through differentiation-independent mechanisms. Am J Physiol Renal Physiol 2005;289:31-42.

11 Broekema M, Harmsen MC, Koerts JA , Petersen AH, van Luyn MJ, Navis G, Popa ER: Determinants of tubular bone marrow-derived cell engraftment after renal ischemia/reperfusion in rats. Kidney Int 2005;68:2572-2581.

12 Morigi M, Imberti B, Zoja C, Corna D, Tomasoni S, Abbate M, Rottoli D, Angioletti S, Benigni A, Perico N, Alison M, Remuzzi G: Mesenchymal stem cells are renotropic, helping to repair the kidney and improve function in acute renal failure. J Am Soc Nephrol 2004;15:1794-1804.

13 Fang TC, Alison MR, Cook HT, Jeffery R, Wright NA, Poulsom R : Proliferation of bone marrow-derived cells contributes to regeneration after folic acid-induced acute tubular injury. J Am Soc Nephrol 2005;16:1723-1732.

14 Fang TC, Otto WR, Jeffery R, Hunt T, Alison MR, Cook HT, Wright NA, Poulsom R: Exogenous bone marrow cells do not rescue non-irradiated mice from acute renal tubular damage caused by HgCl2, despite establishment of chimaerism and cell proliferation in bone marrow and spleen. Cell Prolif 2008;41:592-606.

15 Morigi M, Introna M, Imberti B, Corna D, Abbate M, Rota C, Rottoli D, Benigni A, Perico N, Zoja C, Rambaldi A, Remuzzi A, Remuzzi G: Human Bone Marrow-mesenchymal Stem Cells Accelerate Recovery of Acute Renal Injury and Prolong Survival in Mice. Stem Cells 2008;26:2075-2082.
16 Ma FY, Liu J, Kitching AR, Manthey CL, Nikolic-Paterson DJ: Targeting renal macrophage accumulation via c-fms kinase reduces tubular apoptosis but fails to modify progressive fibrosis in the obstructed rat kidney. Am J Physiol Renal Physiol 2009;296:F177-F185.
17 Gonçalves RG, Biato MA, Colosimo RD, Martinusso CA, Pecly ID, Farias EK, Cardoso LR, Takiya CM, Ornellas JF, Leite M Jr: Effects of mycophenolate mofetil and lisinopril on collagen deposition in unilateral ureteral obstruction in rats. Am J Nephrol 2004;24:527-536.
18 Dolber PC, Spach MS: Conventional and confocal fluorescence microscopy of collagen fibers in the heart. J Histochem Cytochem 1993;41:465-469.
19 de Andrade Pinto AC, Barbosa CM, Ornellas DS, Novaira HJ, de Souza-Menezes J, Ortiga-Carvalho TM, Fong P, Morales MM: Thyroid hormones stimulate renal expression of CFTR. Cell Physiol Biochem 2007;20:83-90.
20 Souza-Meneses J, Tukaye DN, Novaira HJ, Guggino WB, Morales, MM: Small nuclear RNAs U11 and U12 modulate expression of TNR-CFTR mRNA in mammalyan kidneys. Cell Physiol Biochem 2008;22:93-100.
21 Wiese C, Rolletschek A, Kania G, Blyszczuk P, Tarasov KV, Tarasova Y, Wersto RP, Boheler KR, Wobus AM: Nestin expression - a property of multi-lineage progenitor cells? Cell Mol Life Sci 2004;61:2510-2522.
22 Chen J, Boyle S, Zhao M, Su W, Takahashi K, Davis L, Decaestecker M, Takahashi T, Breyer MD, Hao CM: Differential expression of the intermediate filament protein nestin during renal development and its localization in adult podocytes. J Am Soc Nephrol 2006;17:1283-1291.
23 Wagner N, Wagner KD, Scholz H, Kirschner KM, Schedl A: Intermediate filament protein nestin is expressed in developing kidney and heart and might be regulated by the Wilms' tumor suppressor Wt1. Am J Physiol Regul Integr Comp Physiol 2006;291:R779-R787.
24 Zou J, Yaoita E, Watanabe Y, Yoshida Y, Nameta M, Li H, Qu Z, Yamamoto T: Upregulation of nestin, vimentin, and desmin in rat podocytes in response to injury. Virchows Arch. 2006;448:485-492.
25 Oliver J, Maarouf O, Cheema F, Martens TP, Al-Awqati Q: The renal papilla is a niche for adult kidney stem cells. J Clin Invest 2004;114:795-804.
26 Sakairi T, Hiromura K, Yamashita S, Takeuchi S, Tomioka M, Ideura H, Maeshima A, Kaneko Y, Kuroiwa T, Nangaku M, Takeuchi T, Nojima Y: Nestin expression in the kidney with an obstructed ureter. Kidney Int 2007;72:307-318.
27 Yamashita S, Maeshima A, Nojima Y: Involvement of renal progenitor tubular cells in epithelial-to-mesenchymal transition in fibrotic rat kidneys. J Am Soc Nephrol 2005;16:2044-2051.
28 Ishizaki M, Ishiwata T, Adachi A, Tamura N, Ghazizadeh M, Kitamura H, Sugisaki Y, Yamanaka N, Naito Z, Fukuda Y: Expression of nestin in rat and human glomerular podocytes. J Submicrosc Cytol Pathol 2006;38:193-200.
29 Kadler KE, Hill A, Canty-Laird EG: Collagen fibrillogenesis: fibronectin, integrins, and minor collagens as organizers and nucleators. Curr Opin Cell Biol 2008;20:495-501.
30 Bani-Hani AH, Campbell MT, Meldrum DR, Meldrum KK: Cytokines in epithelial-mesenchymal transition: a new insight into obstructive nephropathy. J Urol 2008;80:461-468.
31 Bosan IB: Recommendations for early diagnosis of chronic kidney disease. Ann Afr Med 2007;6:30-136.
32 Chianchiano D: State approaches to stem toll of chronic kidney disease. Adv Chronic Kidney Dis 2008;5:174-176.
33 Watorek E, Klinger M: Stem cells in nephrology: present status and future. Arch Immunol Ther Exp 2006;54:45-50.
34 Burt RK, Loh Y, Pearce W, Beohar N, Barr WG, Craig R, Wen Y, Rapp JA, Kessler J: Clinical applications of blood-derived and marrow-derived stem cells for non-malignant diseases. JAMA 2008;299:925-936.
35 Humphreys BD, Valerius MT, Kobayashi A, Mugford JW, Soeung S, Duffield JS, McMahon AP, Bonventre JV: Intrinsic epithelial cells repair the kidney after injury. Cell Stem Cell 2008;2:284-291.
36 Patschan D, Michutina T, Shi HK, Dolff S, Brodsky SV, Vasilieva T, Cohen-Gould L, Winaver J, Chander PN, Enikolopov G, Goligorsky MS: Normal distribution and medullary-to-cortical shift of nestin-expressing cells in acute renal ischemia. Kidney Int 2007;71:744-754.
37 Daniel C, Albrecht H, Lüdke A, Hugo C: Nestin expression in repopulating mesangial cells promotes their proliferation. Lab Invest 2008;88:387-397.
38 Wang Y, Wang Y, Cai Q, Zheng G, Lee VW, Zheng D, Li X, Tan TK, Harris DC: By homing to the kidney, activated macrophages potently exacerbate renal injury. Am J Pathol 2008;172:1491-1499.
39 Imberti B, Morigi M, Tomasoni S, Rota C, Corna D, Longaretti L, Rottoli D, Valsecchi F, Benigni A, Wang J, Abbate M, Zoja C, Remuzzi G: Insulin-like growth factor-1 sustains stem cell mediated renal repair. J Am Soc Nephrol 2007;18:2921-2928
40 Tögel F, Weiss K, Yang Y, Hu Z, Zhang P, Westenfelder C: Vasculotropic, paracrine actions of infused mesenchymal stem cells are important to the recovery from acute kidney injury. Am J Physiol Renal Physiol 2007;292:1626-1635.
41 Tögel F, Cohen A, Zhang P, Yang Y, Hu Z, Westenfelder C: Autologous and allogeneic marrow stromal cells are safe and effective for the treatment of acute kidney injury. Stem Cells Dev 2009;18:475-485.
42 Fox JM, Chamberlain G, Ashton BA, Middleton J: Recent advances into the understanding of mesenchymal stem cell trafficking. Br J Haematol 2007;137:491-502.
43 Liu Y, Rajur K, Tolbert E, Dworkin LD: Endogenous hepatocyte growth factor ameliorates chronic renal injury by activating matrix degradation pathways. Kidney Int 2000;58:2028-2043.
44 Iwano M, Plieth D, Danoff TM, Xue C, Okada H, Neilson EG: Evidence that fibroblasts derive from epithelium during tissue fibrosis. J Clin Invest 2002;110:341-350.
45 Broekema M, Harmsen MC, van Luyn MJ, Koerts JA, Petersen AH, van Kooten TG, van Goor H, Navis G, Popa ER: Bone marrow-derived myofibroblasts contribute to the renal interstitial myofibroblast population and produce procollagen I after ischemia/reperfusion in rats. J Am Soc Nephrol 2007;18:165-175
46 Li J, Deane JA, Campanale NV, Bertram JF, Ricardo SD: The contribution of bone marrow-derived cells to the development of renal interstitial fibrosis. Stem Cells 2007;25:697-706.
47 Roufosse C, Bou-Gharios G, Prodromidi E, Alexakis C, Jeffery R, Khan S, Otto WR, Alter J, Poulsom R, Cook HT: Bone marrow-derived cells do not contribute significantly to collagen I synthesis in a murine model of renal fibrosis. J Am Soc Nephrol 2006;17:775-782.
48 Ahn KO, Li C, Lim SW, Song HK, Ghee JY, Kim SH, Kim JY, Yoon HE, Cha JH, Kim J, Yang CW: Infiltration of nestin-expressing cells in interstitial fibrosis in chronic cyclosporine nephropathy. Transplantation 2008;86:571-577.